VILNIUS TECH
Vilnius Gediminas Technical University

Proceedings of the 13th International Scientific Conference

ENVIRONMENTAL ENGINEERING

April 23–24, 2026, Vilnius, LITHUANIA

eISSN 2029-7092
eISBN 978-609-476-444-8
Article ID: enviro.2026.1449
https://doi.org/10.3846/enviro.2026.1449

III. GEOSPATIAL TECHNOLOGIES AND INNOVATIONS IN GEODESY, REMOTE SENSING, AND ENVIRONMENTAL MONITORING

http://vilniustech.lt/enviro

COASTAL FLOOD DETECTION IN ŠILUTĖ DISTRICT USING SENTINEL-1 SAR AND COMPARISON WITH MODELED 2022 FLOOD-RISK ZONES

Rokas BRAŽIŪNAS, Jūratė SUŽIEDELYTĖ VISOCKIENĖ*, Eglė TUMELIENĖ, Rosita BIRVYDIENĖ, Arminas STANIONIS

Department of Geodesy and Cadastre, Vilnius Gediminas Technical University, Saulėtekio al. 11, 10223 Vilnius, Lithuania

Received 25 November 2025; revised 31 January 2026; accepted 25 February 2026

Abstract. Flood monitoring and water level change analysis are essential for assessing climate change impacts and managing flood risks. This study aimed to identify flood-affected areas in the Šilutė District using Sentinel-1 SAR change detection and to compare them with modeled flood-risk zones. Sentinel-1 GRD VV-polarized data from February and March 2025 were processed in ESA SNAP and analyzed in QGIS, applying orbit correction, radiometric calibration, speckle filtering, and terrain correction using SRTM DEM. Change detection results were classified into three groups: flooded areas ($\Delta VV \leq -3$ dB), double-bounce/inundated vegetation ($\Delta VV \geq 3$ dB), and non-flooded zones (-3 dB $< \Delta VV \leq 3$ dB). Statistical comparison with official flood probability maps (0.1 %, 1 %, and 10 %) revealed a substantial spatial overlap and general consistency between the detected flood-affected areas and modeled flood hazard zones: the largest flooded areas coincide with the 0.1 % probability zone (31.3 million m^2), decreasing to 26.2 million m^2 in the 10 % zone. Group 2 dominated in high-risk areas, indicating extensive water interaction with vegetation and infrastructure. These findings confirm that Sentinel-1 SAR data provide a reliable and spatially consistent tool for flood analysis and can effectively complement traditional hydrometric networks. Future work will integrate Sentinel-2 multispectral data to improve classification accuracy and enable vegetation impact assessment during inundation events.

Keywords: remote sensing, GIS analysis, change detection, Digital Elevation Model (DEM), flood probability maps.

1. Introduction

Monitoring the water level of surface water bodies such as seas or their parts, rivers or river sections, lakes, ponds, and other artificial reservoirs is a crucial component of environmental protection and the planning of hydrotechnical (hydropower) infrastructure, particularly in the context of climate change. Rising air temperatures increase water evaporation rates and alter the water balance in lakes, ponds, and rivers. Changes in precipitation patterns, including intense rainfall, cause sudden water level fluctuations, often resulting in floods. Prolonged drought periods lower water levels, which can lead to reduced water availability, especially during summer, and negatively affect aquatic biodiversity. More frequent and severe floods, storms, and droughts all necessitate more accurate and continuous monitoring of water level variations.

Given current climate trends, more resilient hydropower infrastructure must be designed to either utilize water resources or protect the environment from harmful water impacts (e.g., dams, levees, canals, embankments, spillways, fish passes, hydroelectric plants, breakwaters, etc.) (Seimas of the Republic of Lithuania, 1997b). Water level changes also influence biodiversity, fish migration, and vegetation. Surface water bodies and their water levels cannot be altered without conducting an environmental impact assessment in accordance with the procedures established by the Law on Environmental Impact Assessment of Planned Economic Activities (Seimas of the Republic of Lithuania, 1996).

To monitor the condition and changes of surface and groundwater bodies across all river basin districts or their parts within the territory of the Republic of Lithuania, water monitoring programs and plans are developed in compliance with the Environmental Monitoring Law (Seimas of the Republic of Lithuania, 1997a). Accurate water level data enable flood modeling and forecasting, reducing damage to nature, life, and property; managing water resources during droughts when water supply becomes limited; and observing long-term climate-related changes, such as sea-level rise or glacier melting.

* Corresponding author. E-mail: *juratesuziedelyte-visockiene@vilniustech.lt*

Water level monitoring methods include hydrometric stations equipped with sensors (typically float-based). In Lithuania, 95 Water Measurement Stations (WMS) currently record hourly water level and temperature data. Additionally, numerous water level monitoring points operate at hydropower facilities, which can be considered supplementary hydrometric stations. However, the spatial distribution of WMS reveals that not all Lithuanian water bodies particularly smaller ones are covered by monitoring, indicating limited geographic coverage. Challenges also include restricted access to water bodies during extreme weather conditions, insufficient data update frequency, and inadequate sensor maintenance.

Modern technologies are fundamentally transforming the possibilities of water level monitoring. Geographic Information Systems (GIS) enable the integration of diverse data sources hydrological, meteorological, topographic, bathymetric, and Digital Elevation Model (DEM) data into unified GIS platforms that facilitate spatial and temporal analysis and visualization of water level changes (Al-Muqdadi & Merkel, 2011; Li, 2019). Researchers emphasize that automated analysis of flat terrain basins remains a challenge and cannot be performed without in-situ measurements. Specialized commercial GIS software, such as River Tools, is widely used for hydrological analysis, particularly for modeling river networks and basins. It offers a broad range of algorithms for assessing water flows, watershed boundaries, river characteristics, and other hydrological parameters. However, applying these algorithms to Shuttle Radar Topography Mission (SRTM) Digital Terrain Model (DTM) data with 90 m spatial resolution provided by NASA and the U.S. Geological Survey (USGS) has revealed limited accuracy and inefficient performance in large-scale analyses (Open Topography, n.d.).

Global Navigation Satellite Systems (GNSS) technologies allow precise measurement of vertical land surface changes, which may be associated with flood risk or shoreline erosion (Awange, 2018; Jiang et al., 2022). Synthetic Aperture Radar (SAR) satellite technology enables monitoring of water bodies regardless of weather conditions or illumination (Chaminé et al., 2021). SAR data are particularly valuable for real-time flood mapping and monitoring. The integration of these technologies makes it possible to develop high-resolution, continuously updated water level monitoring models that are essential for both scientific research and practical water resource management (Singh & Fiorentino, 1996; Suhara & Haghi, 2025).

Ground-based GNSS Interferometric Reflectometry (GNSS-IR) is proposed as a cost-effective method for real-time water level estimation using two inexpensive antennas that receive both the direct GNSS signal from the satellite and the signal reflected from the surface (e.g., water). By analyzing the interference pattern of these signals, the reflector height – corresponding to the water level can be determined. Validation and testing results are compared with pressure sensors installed at the same location, which record flood measurements. It has been observed that GNSS-IR measurements are influenced by local conditions and signal delays caused by the troposphere. This error can be effectively mitigated through signal correction techniques (Purnell et al., 2024). The tropospheric delay effect increases exponentially at lower elevation angles, leading to underestimation of reflector height. This phenomenon in the GNSS-IR context has been studied by Williams and Nievinski (2017) and Nikolaidou et al. (2020, 2023).

Remote sensing data, available almost in real time, are increasingly used for water level monitoring. Sentinel-1, a European Space Agency (ESA) satellite employing SAR technology, enables observation of water surface changes regardless of weather conditions (Farhadi et al., 2025). COSMO-SkyMed, an Italian satellite system, provides high-resolution SAR data suitable for monitoring flood zones and water bodies (Ghosh et al., 2024; Nirchio et al., 2018). CYGNSS (Cyclone GNSS), a NASA mission based on GNSS-R principles, allows monitoring of ocean surface dynamics and inland water bodies (Song et al., 2025).

Advanced data processing techniques enable efficient analysis and prediction of water level variations, flood risk, and land-water boundary dynamics. One of the simplest approaches is classification, used to identify water bodies, flood zones, and land-water boundaries from satellite imagery. Commonly applied indices include WI (Water Index), NDWI (Normalized Difference Water Index), and AWEI (Automated Water Extraction Index), which facilitate rapid detection of flood-affected areas, particularly using Landsat or Sentinel data (Sivanpillai et al., 2021). Classification methods range from traditional algorithms to deep neural networks, which improve accuracy and allow processing of large datasets (Notarangelo et al., 2025).

A more advanced technique is interferometry – SAR interferometry (InSAR) methods detect subtle surface elevation changes associated with flooding, shoreline erosion, or land deformation. Sentinel-1 and COSMO-SkyMed data are frequently used for these purposes. Interferometry enables the creation of high-resolution terrain models and monitoring of vertical displacements with millimeter-level precision (Crosetto & Solari, 2020; Darvishi et al., 2021).

Machine learning is also gaining popularity, with modern algorithms such as LSTM, Random Forest, SVM, and hybrid models applied for water level forecasting and flood risk assessment. These approaches automate data analysis, synthesize information from multiple sources (e.g., meteorological, topographic, satellite), and provide accurate short- and long-term predictions (Asif et al., 2025; Konapala et al., 2021). Furthermore, SHAP analysis can identify the most influential factors contributing to flood probability (Choubin et al., 2025).

The integration of these methods with GIS and

remote sensing technologies forms the foundation for advanced water level monitoring and forecasting solutions, essential for both scientific research and practical water resource management. For such analyses using Copernicus Sentinel satellite data, the European Space Agency (ESA) has developed a free, open-source software platform ESA SNAP (Sentinel Application Platform) designed for remote sensing data processing and analysis (Science Toolbox Exploitation Platform, 2025). The software integrates well with QGIS, one of the most widely used open-source GIS environments (Gandhi, 2025). Using ESA SNAP, satellite data (e.g., Sentinel-1 or Sentinel-2) can be processed, corrected, and analyzed, with results exported to GeoTIFF or other QGIS-compatible formats. This ensures seamless data transfer between applications, enabling further spatial analysis, map creation, and the integration of thematic layers.

This study aims to identify flood-affected areas using Sentinel-1 SAR change detection and to analyze the distribution of terrain elevations within these areas using DEM data.

2. Materials and methods

The research workflow consists of five main stages: import data acquisition, pre-processing and results processing in ESA SNAP, change detection in QGIS, GIS analysis – based comparison with flood-risk maps, and generation of final outputs (Appendix).

The manuscript was linguistically revised and translated using AI-based language support tools (Microsoft Copilot, 2025) to ensure clarity and consistency without altering the scientific content.

2.1. Study areas

Šilutė District was selected as the study area because it is one of the most flood-affected regions in Lithuania and is well-suited for water level monitoring and model application analysis. Located in western Lithuania, the district is unique due to its geographical and hydrological characteristics. It borders the Curonian Lagoon and encompasses the Nemunas Delta region, which is characterized by frequent and severe floods, particularly in spring due to ice drift and snowmelt. This area is identified as a flood risk zone in Lithuania's Flood Risk Management Plan (2023–2027) (European Parliament & Council of the European Union, 2007; Environmental Protection Agency, n.d.), and therefore continuous monitoring and various preventive measures are implemented here. Although hydrometric stations operate in the district, their density is often insufficient for monitoring smaller water bodies or inundated meadows. Consequently, Šilutė District is an appropriate location for applying remote sensing technologies, such as Sentinel-1 SAR, Sentinel-2 optical imagery, GNSS-IR, and DEM models (SRTM 30 m, Copernicus DEM), to accurately identify flood zones and assess changes in water surface elevation. In 2022, an interactive flood hazard and flood risk map was developed for Lithuania for a six-year period, clearly highlighting the flood-related challenges in Šilutė District. These data are presented in Subsection 2.2. Moreover, Šilutė District holds significant ecological and economic importance, with numerous protected areas, fishery farms, and agricultural lands. Therefore, flood impact analysis is highly relevant from environmental, social, and economic perspectives.

2.2. Data sources

The following datasets were used for analyzing coastal flood zones and assessing water surface elevation (Table 1).

Table 1. Research data sources

Data type	Sources	Spatial resolution, m
SRTM DTM	Open Topography (n.d.)	30×30
Sentinel-1 GRD	Copernicus Browser (n.d.)	10×10
Interactive flood hazard and flood risk map (0.1 %, 1.0%, 10% probability)	Environmental Protection Agency (n.d.)	1×1

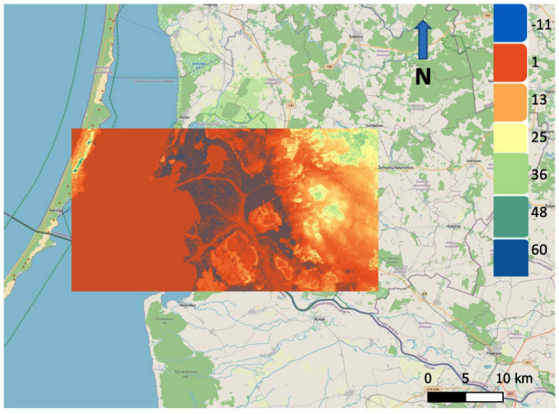

Figure 1. SRTM 30 m elevation data, with legend colors representing heights below sea level (negative values) and above sea level (positive values) in meters (source: authors)

DTM was obtained from the Open Topography platform using the SRTM GL1 (Shuttle Radar Topography Mission Global 1 arc-second) dataset. These data have a spatial resolution of 30 meters (1 arc-second) and cover nearly the entire global territory between 60° N and 56° S latitude. The SRTM data were collected in 2000 during a joint mission of NASA and the United States Geological Survey (USGS) using SAR aboard the Space Shuttle Endeavour. The data were processed and provided as digital elevation models suitable for GIS analyses, hydrological

modeling, flood zone identification, and surface change monitoring. The Open Topography platform enabled the selection of the Šilutė district area via an interactive map and the download of data in GeoTIFF format (Figure 1). SRTM 30 m data serve as the primary terrain source for the terrain correction step when processing Sentinel-1 SAR data in the SNAP environment. In addition, the DEM was used as ancillary data to analyze the distribution of terrain elevations within the detected flooded areas. The analyzed coastal areas of Šilutė District mostly fall within the 0–5 m Above Mean Sea Level (AMSL) elevation range, which makes them highly vulnerable to flood risk.

Sentinel-1 GRD (Ground Range Detected) data are satellite radar images that enable monitoring of Earth's surface changes regardless of weather conditions or illumination. The downloaded GRD products include VV and VH polarization channels, which are particularly useful for identifying flood zones. The data are obtained from the Copernicus Browser (n.d.) and will be processed in the ESA SNAP tools environment, applying orbit correction, noise removal, radiometric calibration, and terrain correction using a DEM. Sentinel-1 imagery will be used to create flood maps and analyze water surface changes over time. For this study, Sentinel-1 GRD data were selected for the winter-spring season: before the expected flood (2025-02-25) and during the flood event (2025-03-07).

The results are compared with coastal maps presenting flood scenarios of low, medium, and high probability (Figures 2a–c). The impacts of snowmelt and heavy rainfall are classified under low (0.1%), medium (1%), and high (10%) flood hazard probabilities (Environmental Protection Agency, n.d.).

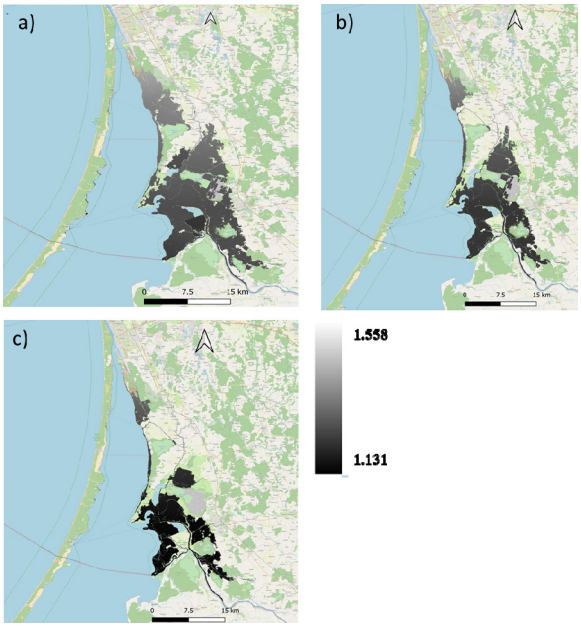

Figure 2. Interactive flood risk map of the Šilutė district: a) consequences of snowmelt and heavy rainfall with a 0.1% probability; b) 1% probability; c) 10% probability (source: Environmental Protection Agency, n.d.; visualization – authors)

2.3. Sentinel-1 GRD data pre-processing

Sentinel-1 GRD data from 2025-02-25 and 2025-03-07 were imported into the ESA SNAP tools for pre-processing (Table 2). In the first step, the satellite orbit information for each product was updated using the Apply Orbit File function. This function replaces preliminary orbital trajectories with precise post-mission orbit data, reducing spatial errors and ensuring the reliability of subsequent processing steps.

Table 2. Sentinel-1 GRD preprocessing settings used in ESA SNAP

Processing step	Setting	Value / Description
Product type	Sentinel-1	GRD, IW mode, VV polarization
Acquisition geometry	Relative orbit	Same relative orbit / track for both dates
Acquisition geometry	Pass direction	Ascending (if true) / Descending
Incidence angle	Range	Within the standard IW swath range (~29°–46°)
Border noise removal	Applied	Yes (GRD border noise removal enabled)
Thermal noise removal	Applied	Yes (default SNAP settings)
Radiometric calibration	Output	Sigma0 (σ^0) backscatter
Speckle filtering	Filter type	Lee filter
Speckle filtering	Window size	5×5 pixels
Terrain correction	DEM	SRTM 30 m
Terrain correction	Pixel spacing	10 m
Terrain correction	Map projection	LKS94 / Lithuania TM
Terrain correction	Resampling method	Bilinear

The next step, thermal noise removal, eliminates thermal noise caused by the radar electronics of the satellite. This noise typically appears as spots or stripes in the image, especially in edge areas where the signal strength is weak, and its removal improves image quality. Further, an essential and mandatory step Radiometric Calibration, which converts image intensity values into physical units. After calibration, different images become comparable as they are expressed in the same units. To reduce speckle graininess caused by coherent radar wave interference the Speckle Filtering step is applied. Although not mandatory, it is recommended as it improves image quality and reduces noise. SAR images exhibit geometric distortions due to the satellite's observation angle and terrain relief. Therefore, Terrain Correction is performed, assigning each pixel its correct spatial position on the map and enabling integration with other GIS datasets. The correction uses a selected

reference modeling this case, SRTM 30 and an appropriate coordinate system (LKS94/Lithuania TM), suitable for Lithuania (Figure 4). For water change assessment, the processed data from different dates are combined into a single Stack in ESA SNAP. Change detection calculations were performed using the following expression:

$$\Delta VV\_line = sigma0\_VV_{\_2025\text{-}03\text{-}07} - sigma0\_VV_{\_2025\text{-}02\text{-}27.} \quad (1)$$

The change detection results were transformed into the dB scale in the QGIS software, which facilitates the interpretation of threshold values. In QGIS, the layer (Band) values in linear units correspond to: Band 1 – VV polarization from the first date (2025-02-27); Band 2 – VV polarization from the second date (2025-03-07).

The changes were calculated using the QGIS Raster Calculator function with the following expression:

$$\Delta VV\_dB = 10 * \log10(\text{„Band2“}) - 10 * \log10(\text{„Band1“}). \quad (2)$$

The difference in decibels (ΔVV_dB) between two radar bands (Sentinel-1 VV polarization data) is calculated. In the formula, the log10 function converts the linear backscatter value into a logarithmic scale, and multiplication by 10 expresses the ratio in decibels. The resulting difference between the two bands indicates relative change (e.g., flooding or surface moisture variations).

Negative ΔVV_dB values indicate a decrease in radar backscatter between the two acquisition dates. Such decreases are typically associated with the presence of smooth open water surfaces, where specular reflection directs most of the radar energy away from the sensor. However, this interpretation should be treated with caution, as backscatter reductions may also result from soil moisture changes or surface smoothing.

Positive ΔVV_dB values represent an increase in radar backscatter. In flood conditions, such increases are commonly related to double-bounce scattering mechanisms, for example when water inundates vegetation or built-up areas containing vertical structures. Increased backscatter may also result from enhanced water-surface roughness caused by wind or wave activity. Therefore, positive ΔVV_dB values are interpreted as inundated vegetation, flooded built-up areas, or roughness-driven water surface changes rather than smooth open water.

3. Results

Sentinel-1 GRD data from 2025-02-25 and 2025-03-07, after terrain correction, represent geocoded radar backscatter (σ^0) values, corrected for geometric distortions using the SRTM 30 m DEM (Figure 3).

Terrain correction ensures accurate spatial alignment of SAR backscatter data with other GIS layers; however, it does not generate elevation information. The elevation data used in this study are derived exclusively from the external SRTM DEM and are treated as ancillary information in subsequent analyses.

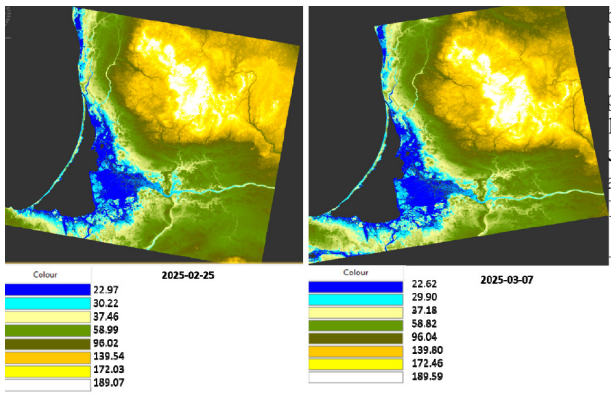

Figure 3. Sentinel-1 GRD VV-polarized backscatter (σ^0) after terrain correction using the SRTM 30 m DEM (source: authors)

This step is crucial because terrain correction eliminates geometric distortions caused by the satellite's observation angle and surface irregularities. As a result, accurate pixel geolocation is ensured, enabling reliable integration with other GIS layers and further spatial analysis. Analysis of the SRTM DEM indicates that large parts of the Šilutė District are located at very low elevations, in some areas close to or below mean sea level.

To assess the topographic characteristics of flood-affected areas, the flooded-area mask derived from Sentinel-1 change detection was overlaid with the DEM, and the distribution of terrain elevations within the detected inundation zones was analyzed.

This provides a fundamental basis for subsequent flood zone analysis and risk assessment. The change detection results (2025-02-27 and 2025-03-07) were simplified by classifying ΔVV_db values into three groups to facilitate interpretation. Values from –99 to –3 dB were assigned to Group 1, representing flooded areas; –3 to 3 dB to Group 3, corresponding to non-flooded zones; and 3 to 999 dB to Group 2, indicating increased backscatter due to double-bounce effects or inundated vegetation. This classification provides a clear distinction between flood-affected areas and stable land (Figure 4).

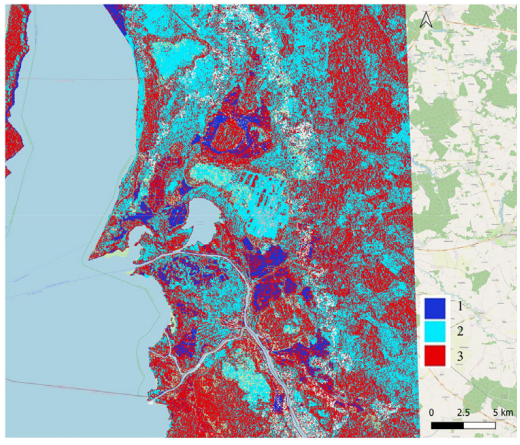

Figure 4. The change detection groups (source: authors)

The results (Figure 5) indicate that the Šilutė District is highly sensitive to flooding. This tendency was verified by comparing the classified change detection output with the coastal *Interactive Flood Risk Map of the Šilutė District* through statistical pixel count analysis. For this purpose, the flood probability maps were resampled to a 10×10 m spatial resolution, and data extents as well as coordinate reference systems were harmonized to ensure accurate overlay and comparison. Statistical analysis in Table 3 and Figure 5.

Table 3. Statistical analysis

Flood Probability Zone	Group 1 (Flooded)	Group 2 (Double Bounce / Vegetation)	Group 3 (Non-flooded)	Total
0.1%	31 285 300	116 039 200	125 441 400	272 765 900
1%	29 888 200	69 351 500	95 784 500	195 024 200
10%	26 200 100	42 041 200	64 771 800	133 013 100

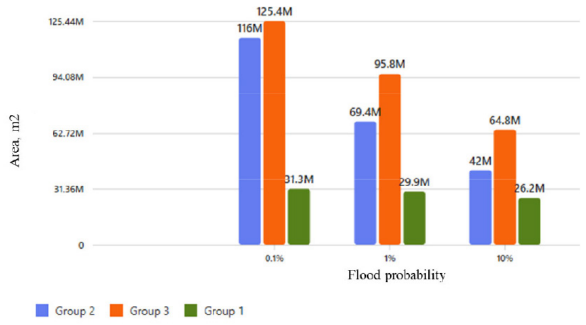

Figure 5. Distribution of classified areas by flood probability zones (0.1%, 1%, and 10%) and Sentinel-1 change detection groups (*M* – million)

Statistical analysis (Table 2) and visual representation (Figure 6) demonstrate the spatial distribution of classified areas across three flood probability zones (0.1%, 1%, and 10%) and their correspondence with Sentinel-1 change detection groups. The largest flooded areas (Group 1) coincide with the 0.1 % probability zone, covering approximately 31.3 million m², while this area decreases to 26.2 million m² in the 10% probability zone. Group 2, associated with double-bounce scattering effects, inundated vegetation, flooded built-up areas, or increased water-surface roughness, inundated vegetation, and flooded built-up areas. Non-flooded areas (Group 3) remain the largest category overall but gradually decrease as flood probability increases. These findings confirm a strong correlation between Sentinel-1 change detection results and official flood risk maps, highlighting the high vulnerability of the Šilutė District to flooding. It should be emphasized that the 0.1%, 1%, and 10% flood hazard maps represent long-term flood probability scenarios rather than the actual extent of a specific flood event. Therefore, the comparison is intended to assess general spatial consistency rather than to provide direct validation of the Sentinel-1 results.

The presented flood detection results are not independently validated due to the lack of spatially explicit ground truth data for the analyzed event. Therefore, the results should be interpreted as indicative flood-extent patterns derived from SAR backscatter changes rather than as a definitive representation of actual inundation.

4. Conclusions

The study demonstrated that Sentinel-1 SAR change detection, integrated with DEM, is an effective approach for identifying flood-affected areas in low-lying coastal regions. Terrain correction ensured accurate geolocation and enabled reliable integration with GIS datasets.

Change detection between February and March 2025 revealed significant backscatter variations, which were classified into three groups: flooded areas ($\Delta VV \leq -3$ dB), double-bounce/inundated vegetation ($\Delta VV \geq 3$ dB), and non-flooded zones (-3 dB $< \Delta VV \leq 3$ dB). This classification provided a clear spatial distinction between inundated and stable land.

Comparison with official flood hazard maps indicates a general spatial consistency between the Sentinel-1 detected flood-affected areas and zones of higher modeled flood hazard. The largest flooded areas coincide with the 0.1% probability zone (31.3 million m²), decreasing to 26.2 million m² in the 10% zone. Group 2 dominated in the highest-risk areas, indicating extensive water interaction with vegetation and infrastructure.

These findings highlight the high vulnerability of the Šilutė District to flooding and demonstrate that Sentinel-1 SAR data can complement traditional hydrometric networks, offering near-real-time, spatially consistent flood monitoring capabilities.

In future research, Sentinel-2 multispectral data will be integrated with Sentinel-1 SAR observations to enhance flood detection accuracy and enable the assessment of vegetation and land cover changes during inundation events. Combining radar and optical datasets will allow for more robust classification, improved discrimination between water and wet soil, and the development of advanced machine learning models for flood risk prediction.

It should be noted that SAR backscatter over water surfaces is influenced not only by inundation but also by environmental conditions. Wind-induced surface roughness can significantly increase VV backscatter over water, potentially leading to positive ΔVV values even in the absence of vegetation or built structures. In addition, seasonal factors such as snowmelt, ice cover, and early-spring soil moisture conditions may affect radar backscatter responses and should be considered when interpreting change detection results.

References

Al-Muqdadi, S. W., & Merkel, B. J. (2011). Automated watershed evaluation of flat terrain. *Journal of Water Resource and Protection*, *3*(12), 892–903. https://doi.org/10.4236/jwarp.2011.312099

Asif, M., Kuglitsch, M. M., Pelivan, I., & Albano, R. (2025). Review and intercomparison of machine learning applications for short-term flood forecasting. *Water Resources Management*, *39*, 1971–1991. https://doi.org/10.1007/s11269-025-04093-x

Awange, J. (2018). *GNSS environmental sensing*. Springer. https://doi.org/10.1007/978-3-319-58418-8

Chaminé, H. I., Pereira, A. J. S. C., Teodoro, A. C., & Teixeira, J. (2021). Remote sensing and GIS applications in earth and environmental systems sciences. *SN Applied Sciences*, *3*, Article 870. https://doi.org/10.1007/s42452-021-04855-3

Choubin, B., Jaafari, A., Henareh, J., Karimi, O., & Sajedi Hosseini, F. (2025). Explainable artificial intelligence (XAI) for interpreting predictive models and key variables in flood susceptibility. *Results in Engineering*, *27*, Article 105976. https://doi.org/10.1016/j.rineng.2025.105976

Copernicus Browser. (n.d.). https://browser.dataspace.copernicus.eu/

Crosetto, M., & Solari, L. (2020, March 22–26). Deformation monitoring using satellite radar interferometry. In *Proceedings of the 2020 IEEE Latin American GRSS & ISPRS Remote Sensing Conference* (*LAGIRS*), (pp. 240–245). Santiago, Chile. IEEE. https://doi.org/10.1109/LAGIRS48042.2020.9165659

Darvishi, M., Destouni, G., Aminjafari, S., & Jaramillo, F. (2021). Multi-Sensor InSAR assessment of ground deformations around lake mead and its relation to water level changes. *Remote Sensing*, *13*(3), Article 406. https://doi.org/10.3390/rs13030406

European Parliament & Council of the European Union. (2007). *Directive 2007/60/EC of the European Parliament and of the Council of 23 October 2007 on the Assessment and Management of Flood Risks* (2007, October 23, No. 32007L0060). Official Journal of the European Union, L 288/27. http://data.europa.eu/eli/dir/2007/60/oj

Environmental Protection Agency. (n.d.). *Flood Risk Management Plan 2023–2027* [Potvynių rizikos valdymo planas 2023–2027 m.]. https://aaa.lrv.lt/lt/veiklos-sritys/vanduo/upes-ezerai-ir-tvenkiniai/potvyniu-rizikos-valdymas/potvyniu-rizikos-valdymo-planas-2023-2027-m/

Farhadi, H., Kiani, A., Ebadi, H., & Asgary, A. (2025). Development of an automatic time-series flood mapping framework using Sentinel-1 and 2 imagery. *Stochastic Environmental Research and Risk Assessment*, *39*(6), 2627–2655. https://doi.org/10.1007/s00477-025-02987-1

Gandhi, U. (2025). *QGIS tutorials and tips*. https://www.qgistutorials.com/en/

Ghosh, B., Garg, S., Motagh, M., & Martinis, S. (2024). Automatic flood detection from Sentinel-1 data Using a Nested UNet model and a NASA benchmark dataset. *PFG – Journal of Photogrammetry, Remote Sensing and Geoinformation Science*, *92*, 1–18. https://doi.org/10.1007/s41064-024-00275-1

Jiang, Z., Hsu, Y.-J., Yuan, L., Feng, W., Yang, X., & Tang, M. (2022). GNSS2TWS: An open-source MATLAB-based tool for inferring daily terrestrial water storage changes using GNSS vertical data. *GPS Solutions*, *26*, Article 114. https://doi.org/10.1007/s10291-022-01301-8

Konapala, G., Kumar, S. V., & Khalique Ahmad, S. (2021). Exploring Sentinel-1 and Sentinel-2 diversity for flood inundation mapping using deep learning. *ISPRS Journal of Photogrammetry and Remote Sensing*, *180*, 163–173. https://doi.org/10.1016/j.isprsjprs.2021.08.016

Li, X. (2019). Application of GIS in hydrologic information forecasting. *Journal of Geographical Research*, *2*(1), 30–33. https://doi.org/10.30564/jgr.v2i1.470

Microsoft 365 Copilot. (2025). [Computer software] (Version June 20). https://copilot.microsoft.com

Nikolaidou, T., Santos, M. C., Williams, S. D. P., & Geremia-Nievinski, F. (2020). Raytracing atmospheric delays in ground-based GNSS reflectometry. *Journal of Geodesy*, *94*, Article 68. https://doi.org/10.1007/s00190-020-01390-8

Nikolaidou, T., Santos, M. C., Williams, S. D. P., & Geremia-Nievinski, F. (2023). Development and validation of comprehensive closed formulas for atmospheric delay and altimetry correction in ground-based GNSS-R. *IEEE Transactions on Geoscience and Remote Sensing*, *61*, Article 5801007. https://doi.org/10.1109/TGRS.2023.3260243

Nirchio, F., Grieco, G., Migliaccio, M., & Nicolosi, P. D. M. (2018). Oil spill monitoring in the Italian waters: COSMO-SkyMed role and contribution. In A. Carpenter & A. G. Kostianoy (Eds.), *Oil Pollution in the Mediterranean Sea*: *Part II*: *National Case Studies* (Vol. 84, pp. 73–95). Springer. https://doi.org/10.1007/698_2016_115

Notarangelo, N., Wirion, C., & van Winsen, F. (2025). STURM-Flood: A curated dataset for deep learning-based flood extent mapping leveraging Sentinel-1 and Sentinel-2 imagery. *Big Earth Data*, *9*(3), 412–438. https://doi.org/10.1080/20964471.2025.2458714

Open Topography. (n.d.). https://opentopography.org

Purnell, D., Gomez, N., Minarik, W., & Langston, G. (2024). Real-time water levels using GNSS-IR: A potential tool for flood monitoring. *Geophysical Research Letters*, *51*(5), Article e2023GL105039. https://doi.org/10.1029/2023GL105039

Science Toolbox Exploitation Platform. (2025). *SNAP*. https://step.esa.int/main/toolboxes/snap/

Seimas of the Republic of Lithuania. (1996). *Law on Environmental Impact Assessment of Planned Economic Activities* [Lietuvos Respublikos planuojamos ūkinės veiklos poveikio aplinkai vertinimo įstatymas] (1996, August 15, No. I-1495). https://e-seimas.lrs.lt/portal/legalAct/lt/TAD/TAIS.30545/asr

Seimas of the Republic of Lithuania. (1997a). *Law on Environmental Monitoring of the Republic of Lithuania* (1997, November 20, No. VIII-529). https://e-seimas.lrs.lt/portal/legalAct/lt/TAD/TAIS.47236/asr

Seimas of the Republic of Lithuania. (1997b). *Law on Water of the Republic of Lithuania* [Lietuvos Respublikos vandens įstatymas] (1997, October 21, No. VIII-474). https://e-seimas.lrs.lt/portal/legalAct/lt/TAD/TAIS.45987/asr

Singh, V. P., & Fiorentino, M. (Eds). (1996). *Geographical Information Systems in Hydrology* (Vol. 26). Springer. https://doi.org/10.1007/978-94-015-8745-7

Sivanpillai, R., Jacobs, K. M., Mattilio, C. M., & Piskorski, E. V. (2021). Rapid flood inundation mapping by differencing water indices from pre- and post-flood Landsat images. *Frontiers of Earth Science*, *15*, 1–11. https://doi.org/10.1007/s11707-020-0818-0

Song, S., Zhu, Y., Qu, X., & Tao, T. (2025). Spaceborne GNSS-R for sensing soil moisture using CYGNSS considering land cover type. *Water Resources Management*, *39*, 3499–3519. https://doi.org/10.1007/s11269-025-04119-4

Suhara, K. K., S., & Haghi, A. K. (2025). Applications of GIS and remote Sensing in Hydrology, Water Resource Management and Sustainable Development. In *GIS in Environmental Engineering*: *Core Concepts for Sustainable Development* (pp. 1–25). Springer. https://doi.org/10.1007/978-3-031-79126-0_1

Williams, S. D. P., & Nievinski, F. G. (2017). Tropospheric delays in ground-based GNSS multipath reflectometry – experimental evidence from coastal sites. *Journal of Geophysical Research*: *Solid Earth*, *122*(3), 2310–2327. https://doi.org/10.1002/2016JB013612

APPENDIX

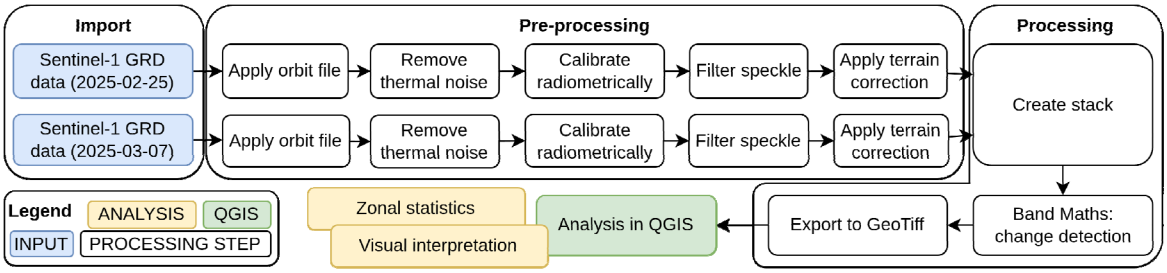

Figure A1. Sentinel-1 GRD data processing scheme